Available online at www.sciencedirect.com
ScienceDirect
Journal of Power Sources 175 (2008) 159–165
JOURNAL OF POWER SOURCES
www.elsevier.com/locate/jpowsour

Methanol oxidation on carbon-supported Pt–Ru–Ni ternary nanoparticle electrocatalysts

Juanying Liu [a,b], Jianyu Cao [a,b], Qinghong Huang [a], Xiaowei Li [a], Zhiqing Zou [a], Hui Yang [a,*]

[a] *Energy Science and Technology Laboratory, Shanghai Institute of Microsystem and Information Technology, Chinese Academy of Sciences, Shanghai 200050, PR China*
[b] *Graduate University of the Chinese Academy of Sciences, Beijing 100039, PR China*

Received 23 July 2007; accepted 31 August 2007
Available online 6 September 2007

Abstract

Methanol oxidation on carbon-supported Pt–Ru–Ni ternary alloy nanoparticles was investigated based on the porous thin-film electrode technique and compared with that on Johnson–Matthey Pt–Ru alloy catalyst. Emphasis is placed on the effect of alloying degree on the electrocatalytic activity and stability of the ternary catalysts. The as-prepared Pt–Ru–Ni nanoparticles exhibited a single phase fcc disordered structure, and a typical TEM image indicates that the mean diameter is ca. 2.2 nm, with a narrow particle size distribution. Also, the as prepared Pt–Ru–Ni catalysts exhibited significantly enhanced electrocatalytic activity and good stability for methanol oxidation in comparison to commercial Pt–Ru catalyst available from Johnson–Matthey. The highest activity of methanol oxidation on Pt–Ru–Ni catalysts was found with a Pt–Ru–Ni atomic ratio of 60:30:10 and at a heat-treatment temperature of ca. 175 °C. The significantly enhanced catalytic activity for methanol oxidation is attributed to the high dispersion of the ternary catalyst, to the role of Ni as a promotion agent, and especially to the presence of hydroxyl Ru oxide. Moreover, the stability of the ternary nanocatalytic system was found to be greatly improved at heat-treatment temperatures higher than ca. 250 °C, likely due to a higher alloying degree at such temperatures for the ternary catalysts.

Keywords: Methanol oxidation; Electrocatalysis; Alloy nanoparticle; Hydroxyl Ru oxide; Stability

1. Introduction

During the last decade, there has been an increasing interest in the development of direct methanol fuel cells (DMFCs) for applications in transportation and in portable electronic devices [1–4]. The use of methanol as a fuel has several advantages in comparison to the use of hydrogen: inexpensive liquid fuel; ease of handling, transport and storage; as well as high theoretical energy density [5,6]. However, the performances of DMFCs are still limited by several problems, including the poor kinetics of both the anodic and cathodic reactions [6–9] and the cross-over of methanol through the proton exchange membrane from the anode to the cathode [1,5].

The oxidation of methanol on Pt-based electrocatalysts has been extensively studied for more than 30 years. Platinum has been found to be the best single-metal catalyst for this reaction, but the formation of linearly adsorbed CO species is found to poison the electrode surface, inhibiting the oxidation reaction. A convenient method of modifying the electrocatalytic properties of platinum in order to reduce or avoid the poisoning effect is the alloying of platinum with the other metals, such as Ru, Sn, W, Mo, Os and Ni. The presence of a second alloying component can increase the activity of platinum-based catalysts through either electronic effects or by way of a bifunctional mechanism in which platinum dissociates methanol by chemisorption and the second component activates water so that oxygen-containing species are formed at lower potentials, thus facilitating the overall reactions on the catalysts. In order to improve the catalytic performance and to decrease the poisoning effect of anode catalysts, many investigations have been conducted on the development of Pt-based binary catalysts, such as Pt–Ru [10–16], Pt–W [17,18], Pt–Mo [19], Pt–Sn [19–21], and Pt–Os [8,22]. From such investigations, it has been ascertained that Pt–Ru systems, due to the bifunctional mechanism

* Corresponding author. Tel.: +86 21 32200534; fax: +86 21 32200534.
E-mail address: hyang@mail.sim.ac.cn (H. Yang).

0378-7753/$ – see front matter © 2007 Elsevier B.V. All rights reserved.
doi:10.1016/j.jpowsour.2007.08.100

and electronic effect [10,11,23] are very effective anode catalysts for methanol oxidation.

To be more precise, according to the bifunctional mechanism at least three Pt atoms are needed to activate one methanol molecule to form a Pt-$(CO)_{ad}$ and one Ru atom is needed to activate one water molecule to form Ru–OH. Thus, the best atomic ratio of Pt to Ru should be 4:1 [16,24,25]; however, the commonly used atomic ratio with Pt:Ru catalysts is found in a range between ca. 4:1 and 1:1 [26,27]. The role of Ru species within the Pt–Ru system has been clarified even more by recent experiments [14,28–30] that show that hydrous Ru oxide is both an active component for oxidation of the carbonaceous intermediates absorbed on Pt surfaces and, also, a mixed proton/electron conductor [14,31]. Conflicting results, however, have been reported that suggest that hydrous ruthenium oxide plays a major role in processes that cause chemical instability in the methanol oxidation process and that the alloy phase is the only phase that enables both electronic interaction and the bifunctional mechanism to work simultaneously [32]. Despite the controversies, recent studies have shown that the addition of Ni to Pt and Pt–Ru catalysts can enhance electrocatalytic activity for methanol oxidation [9,33,34]. For example, Park et al. [33,34] found that carbon-supported Pt/Ni and Pt/Ru/Ni alloys show excellent catalytic activities for methanol oxidation compared to those of Pt and Pt/Ru, respectively; the role of Ni is that of a catalytic enhancing agent. Wang et al. [9] used a combinatorial approach to investigate the optimum composition of a Pt–Ru–Ni system; the best performance for methanol oxidation was found with a Pt–Ru–Ni atomic ratio of 6:3:1. Martinez-Huerta et al. discussed the effect of Ni addition to PtRu/C catalysts on CO and methanol oxidation reaction [35]. And, more recently, Zhang et al. [36] synthesized a Pt–Ru–Ni/C nanocomposite via a microwave-irradiated polyol reduction route. The resulting improved CO-tolerant performance of the nanocomposite was attributed to hydrogen spillover on the catalyst surface, high proton and electronic conductivity of the hydroxides, and enhanced oxidation of CO_{ads} by nickel hydroxides. However, no paper deals with the effect of alloying degree on the activity and stability of methanol oxidation on the Pt–Ru–Ni ternary catalysts.

In the present paper, carbon-supported Pt–Ru–Ni ternary alloy nanoparticles have been prepared using the previously employed carbonyl route [37]. The effects of atomic compositions and heat-treatment temperatures on catalyst activity and stability for methanol oxidation have been examined, and we deduce that the presence of alloys of Pt, Ru and Ni is required in order to rationalize the behavior of the catalytic system when used for methanol oxidation.

2. Experiment

2.1. Preparation of carbon-supported Pt–Ru–Ni alloy nanoparticle catalysts

Nanosized Pt–Ru–Ni ternary alloy nanoparticle catalysts were prepared via a carbonyl route. Resultant powders were heat treated by H_2 reduction in the temperature range of 150–300 °C. In brief, the procedure involved mixing $Na_2PtCl_6{\cdot}6H_2O$, $RuCl_3$ and $NiCl_2{\cdot}6H_2O$ ultrasonically in pure methanol. Sodium acetate was added to this mixture with a sodium acetate/Pt molar ratio of 6:1. This was followed by reacting the mixture with CO at about 50 °C for 24 h until the solution turned green. After the synthesis of the carbonyl complexes, Vulcan XC-72 carbon was added under N_2 gas flow, and the mixture stirred at about 55 °C for more than 6 h. Subsequently, the solvent was removed and the powder was subjected to heat treatment at different temperatures ranged from 150 to 300 °C under nitrogen for 1 h and under hydrogen for 2 h, respectively. After heat treatment, the sample was washed with water until no chlorine ions were detected in the supernatant and then dried under nitrogen at about 120 °C for more than 5 h. The total metal loading of all the carbon-supported catalysts was set at about 20 wt.%.

2.2. Physical characterization of the nanosized Pt–Ru–Ni/C alloy catalysts

The analysis of the atomic composition of the catalysts was performed with an IRIS Advantage inductively coupled plasma atomic emission spectroscopy (ICP-AES) system (Thermo America). X-ray diffraction (XRD) measurements utilized a Rigaku D/MAX-2000 diffractometer with a Cu $K\alpha_1$ radiation (1.54056 Å); the tube voltage was maintained at 40 kV and tube current at 100 mA. Diffraction patterns were collected from 10° to 90° at a scanning rate of 1° min^{-1}, and with a step size of 0.02°. The identification of the phases was made by referring to the Joint Committee on Powder Diffraction Standards - International Center for Diffraction Data (JCPDS-ICDD) database. The particle size of the as-prepared catalysts was evaluated by transmission electron microscopy (TEM), using a Technai G^2 20s-Twin microscope (FEP, Inc., USA).

2.3. Preparation of porous electrode and electrochemical measurements

Porous electrodes were prepared as described previously. Briefly, 10 mg of catalysts, 2.5 ml of water and 0.5 ml of Nafion solution (5 wt.%, Aldrich) were mixed ultrasonically. A measured volume (ca. 3 μl) of this ink was transferred via a syringe onto a freshly polished glassy carbon disk (GC, 3 mm in diameter), and the solvent was evaporated overnight at room temperature. Each electrode contained about 28 μg cm^{-2} of the metal.

All chemicals used were of analytical grade. All solutions were prepared with ultrapure water with a specific resistance of >18 MΩ cm^{-1}. Electrochemical measurements were performed using an M273A Potentiostat/Galvanostat (Princeton, USA) and a conventional three-electrode electrochemical cell. The counter electrode was a glassy carbon plate, and a saturated calomel electrode (SCE) was used as the reference electrode. Potentials quoted herein are with respect to SCE. The electrolyte used was 0.5 M H_2SO_4 or 0.5 M CH_3OH + 0.5 M H_2SO_4 solution. Prior to the electrochemical measurements, the porous electrode was cycled at 20 mV s^{-1} between −0.20 and 0.60 V/SCE in 0.5 M H_2SO_4 solution until a reproducible cyclic voltammogram (CV) was obtained (ca. 15 cycles), in order to remove any contam-

inants from the electrode. High-purity nitrogen was used for deaeration of the solutions, and during measurements a nitrogen flow was maintained above the electrolyte solution.

All experiments were carried out at a temperature of $25 \pm 1\,^{\circ}C$.

3. Results and discussion

3.1. Characterization of the Pt–Ru–Ni/C catalysts of different atomic compositions

To explore the possible effect of atomic composition of the catalysts on their activity, carbon-supported catalysts with different Pt–Ru–Ni atomic ratios, i.e. Pt–Ru–Ni (67.5:22.5:10)/C; Pt–Ru–Ni(60:30:10)/C; and Pt–Ru–Ni(50:40:10)/C were prepared, all with the Ni atomic content chosen as 10%. The practical composition of the ternary catalysts was evaluated by ICP-AES analysis. The ICP-AES compositions for all the catalysts were found to be nearly the same as the stoichiometric values.

Fig. 1a shows the XRD patterns of the carbon-supported Pt–Ru–Ni ternary catalysts, heat treated at 175 °C, with a metal loading of 20 wt.% and with different Pt/Ru/Ni atomic ratios. For reference, the XRD pattern for commercial Pt–Ru(1:1)/C catalyst from Johnson–Matthey (J–M, 20 wt.%) is also provided in the figure. The first peak located at ca. 25° in all the XRD patterns is attributable to the carbon support. The other peaks are characteristics of face-centered-cubic (fcc) crystalline Pt (JCPDS, Card No. 04-802), and are indexed with planes (1 1 1), (2 0 0), (2 2 0) and (3 1 1), at 2θ values of ca. 39°, 47°, 67° and 83°, respectively. This finding indicates that all the catalysts are principally single-phase disordered structures (i.e., solid solutions). Compared to the same reflections in bulk Pt, the diffraction peaks for the ternary catalysts are shifted very slightly to higher 2θ values, probably indicating the formation of an alloy involving Ru and Ni substituted into the fcc structure of Pt, and revealing the effect of various amounts of Ru and Ni in the ternary catalysts. The lattice parameters (a_{fcc}) for the Pt–Ru–Ni catalysts, calculated using the (1 1 1) crystal faces, are provided in Table 1. The lattice parameters for the three Pt–Ru–Ni/C catalysts are only slightly smaller than that for Pt, indicating a slight lattice contraction with increasing content of Ru and Ni. However, the lattice parameters for these three Pt–Ru–Ni/C catalysts are larger than that of the commercial Pt–Ru/C catalyst, indicating that the degree of alloying for these samples (heat treated at 175 °C) is below that of the commercial catalyst. The measured

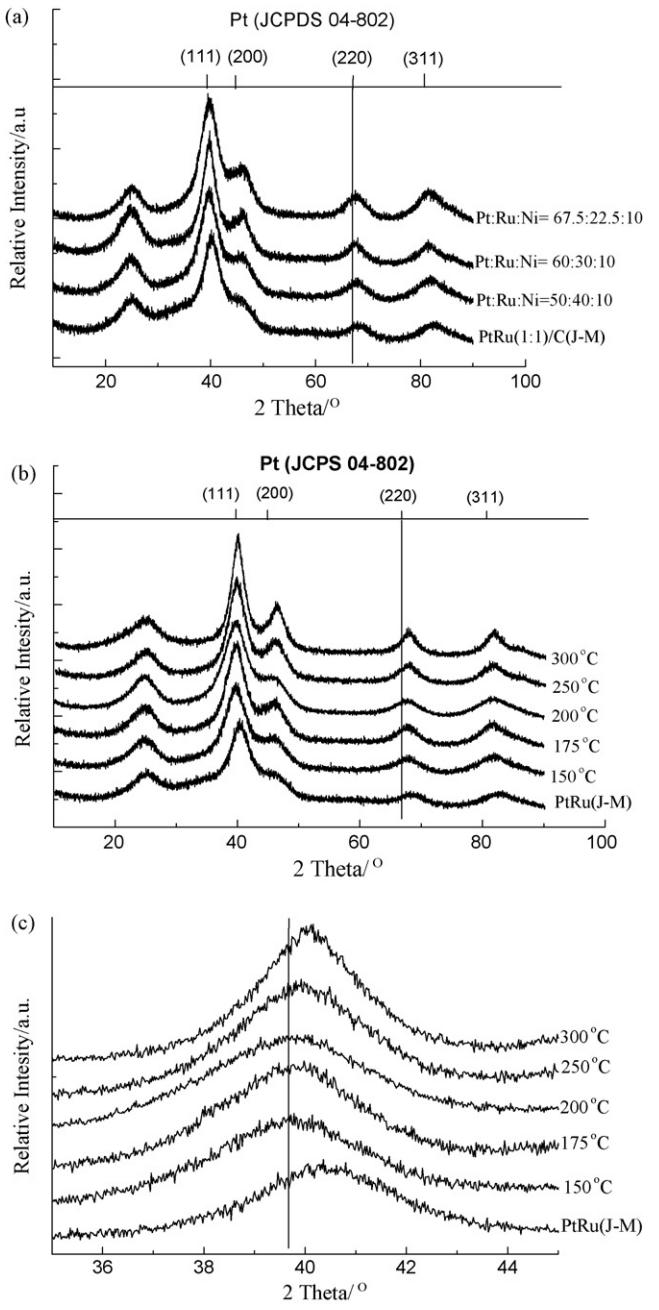

Fig. 1. XRD patterns of (a) the catalysts with different atomic compositions heat treated at 175 °C, (b) the Pt–Ru–Ni(6:3:1)/C alloy catalysts heat treated at various temperatures, and (c) fine scanning of the (1 1 1) peak in (b).

Table 1
Structural parameter and particle size of the Pt–Ru–Ni/C alloy catalysts and the PtRu/C(Johnson–Matthey) catalyst with 20 wt.% metal loading

Catalyst	Lattice parameter (nm)	Particle size (nm) from XRD
Pt–Ru–Ni (67.5:22.5:10)	0.3915	1.8
Pt–Ru–Ni (60:30:10)	0.3924	1.9
Pt–Ru–Ni (50:40:10)	0.3915	2.0
PtRu/C(J–M)	0.3889	1.9

change in lattice parameter with (Ru + Ni) content (see Table 1) does not exhibit Vegard's law behavior for a solid solution. This may be due to the small particle sizes of the as-synthesized samples and the presence of hydrous Ru oxides within our samples (see description below). The average particle sizes are given in Table 1 as estimated using Scherrer's equation. Obviously, all the catalysts have nearly the same structures and similar particle sizes. Thus, under these conditions, comparing electrocatalytic activity for methanol oxidation would be justified.

Fig. 1b is the XRD patterns for Pt–Ru–Ni(60:30:10)/C catalysts heat treated at various temperatures; as in Fig. 1a there are

Table 2
Lattice parameter and particle size of Pt–Ru–Ni/C alloy catalysts and PtRu/C catalyst (Johnson–Matthey) with 20 wt.% metal loading

Heat-treatment temperature (°C)	Lattice parameter (nm)	Particle size (nm) from XRD	Onset potential (mV)
150	0.3925	1.7	52
175	0.3924	1.9	28
200	0.3921	2.1	10
250	0.3908	2.2	53
300	0.3901	2.5	70
PtRu/C(J–M)	0.3889	1.9	94

also five main diffraction peaks for carbon supported Pt–Ru–Ni catalysts that have been heat treated at various temperatures. With increase in heating temperature, diffraction peaks are found to shift slightly to higher angle relative to pure Pt, as is clearly revealed for the (1 1 1) reflection shown in Fig. 1c. The angle shifts reveal alloy formation for Pt, Ru and Ni with increase in heating temperature, and indicate lattice contractions, caused by the incorporation of both Ru and Ni into the Pt fcc structure. Additionally, the lattice parameters (a_{fcc}) for the Pt–Ru–Ni catalysts in Table 2, calculated using the (1 1 1) crystal faces, decrease with the increase in heating temperature. One finds that angle shift increases (and related lattice parameter decreases) with increase in heating temperature suggesting an increased degree of alloying. Although no reflections corresponding to pure Ru and Ni, and their oxides are found in Fig. 1, their presence may not be completely ruled out because of their possible low concentration levels and possibly poor crystallinity. The mean particle sizes calculated from XRD patterns for the synthesized catalysts are shown in Table 2; the mean particle size generally increases with heat-treatment temperature.

Fig. 2 shows a typical TEM image of the carbon-supported Pt–Ru–Ni (60:30:10) alloy catalyst heat treated at 175 °C and the corresponding particle size distribution histogram based on the observation of more than 500 nanoparticles. As can be seen, the Pt–Ru–Ni alloy nanoparticles are well dispersed on the surface of the support with a very narrow size distribution. The obtained mean particle diameter is about 2.2 ± 0.8 nm, which is in fairly good agreement with the data calculated from XRD. The TEM images of the other nanosized catalysts are similar to that shown in Fig. 2 (not shown in the paper), which confirm that the catalyst preparation procedure via carbonyl route is a good method to obtain nanosized ternary alloy catalysts with a narrow particle size distribution and thus a good dispersion.

3.2. Methanol oxidation on Pt–Ru–Ni/C catalysts with different atomic compositions

Fig. 3 shows the CVs of as-prepared Pt–Ru–Ni catalysts with different atomic compositions and heat treated at 175 °C at a scan rate of 20 mV s^{-1} in 0.5 M H_2SO_4 solution; also shown is the CV for a commercial catalyst. The current density in the hydrogen region decreases with increase in (Ru + Ni) weight percent within our samples, indicative of a change in electrochemical active surface area with (Ru + Ni) content; the hydrogen adsorption/desorption area changes in the order of Pt–Ru–Ni(67.5:22.5:10)/C > Pt–Ru–Ni(60:30:10)/C > Pt–Ru–Ni(50:40:10)/C > PtRu/C(J–M). However, no well-defined H adsorption/desorption peaks were found for any of the samples, suggesting that the high dispersion of the catalysts with disordered surface structure was obtained.

Fig. 4 is a comparison of methanol oxidation using the as-prepared Pt–Ru–Ni catalysts of different atomic compositions and heat treatment at 175 °C, as well as that for the commercial Pt–Ru alloy catalyst; where all measurement were acquired at a scan rate of 20 mV s^{-1} in 0.5 M CH_3OH + 0.5 M H_2SO_4. The onset potentials for methanol

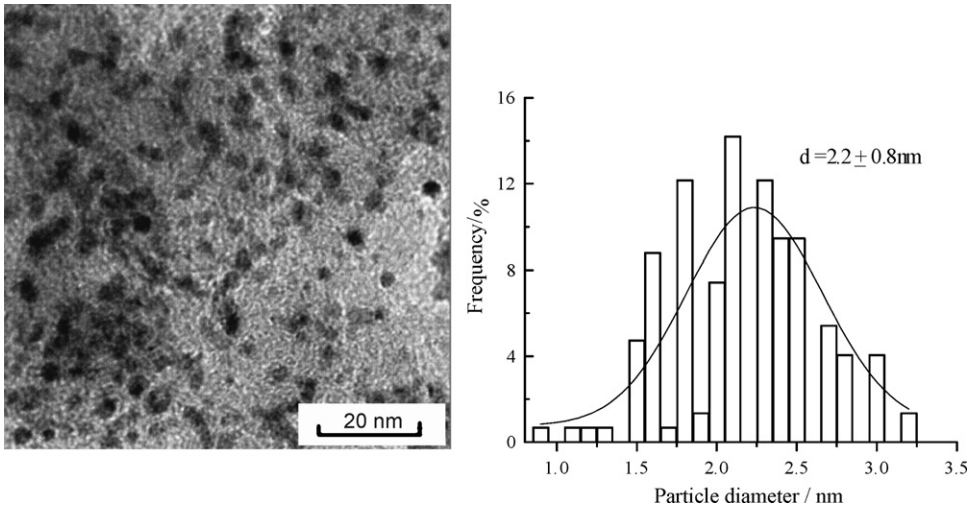

Fig. 2. TEM image of the Pt–Ru–Ni(6:3:1)/C catalyst heat treated at 175 °C, and the corresponding particle size distribution histogram.

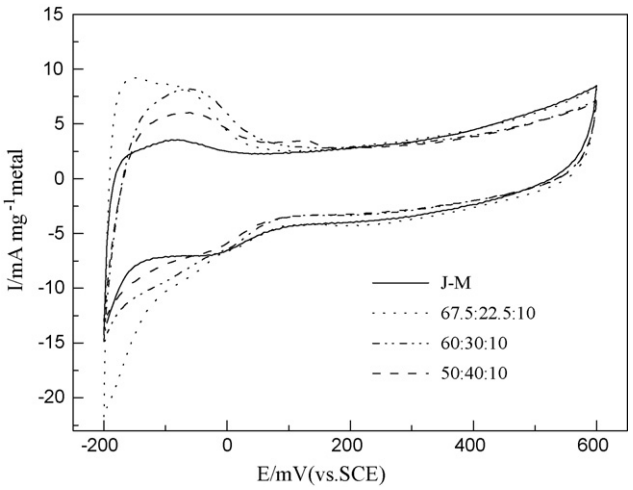

Fig. 3. CVs of as-prepared Pt–Ru–Ni catalysts with different atomic compositions heat treated at 175 °C, and the commercial catalyst at a scan rate of 20 mV s^{-1} in 0.5 M H_2SO_4 solution at 25 ± 1 °C.

oxidation on the in-house synthesized catalysts are slightly lower than that for the commercial Pt–Ru catalyst, indicating an enhanced catalytic activity for methanol oxidation. Methanol oxidation current densities decrease in the order of Pt–Ru–Ni(60:30:10)/C > Pt–Ru–Ni(67.5:22.5:10)/C > Pt–Ru–Ni(50:40:10)/C > PtRu/C, indicating that the Pt–Ru–Ni(60:30:10)/C is the most active among the catalysts investigated. In addition, we also prepared carbon supported Pt–Ru(1:1) alloy catalyst with a metal loading of 20 wt.% by the same procedure described herein; we found its mean particle size from XRD to be ca. 1.8 nm and that its electrocatalytic activity for methanol oxidation is comparable to that of the commercial Pt–Ru(1:1)/C catalyst. Hence, we deduce that enhanced electrocatalytic activity for methanol oxidation on the ternary alloy catalysts is due to the addition of Ni species into Pt–Ru alloy catalysts and to the composition and electronic effects [9,33–35].

3.3. Effect of heat-treated temperatures on the Pt–Ru–Ni/C catalyst activity and stability

To explore the effects of possible different Ru species within the as-synthesized Pt–Ru catalyst system as well as possible changes in the degree of alloying within the catalyst on the catalytic activity and stability for methanol oxidation, the Pt–Ru–Ni(60:30:10)/C catalyst was subjected to heat treatment at various temperatures. As shown earlier in Fig. 1b and c, the alloying degree of the catalysts was found to successively increase with heat-treatment temperature. Fig. 5 shows the CVs of methanol oxidation on the Pt–Ru–Ni(6:3:1)/C alloy catalysts heat treated at various temperatures at a scan rate of 20 mV s^{-1} in 0.5 M CH_3OH + 0.5 M H_2SO_4. It is found that all the in-house synthesized catalysts exhibit lower onset potentials for methanol oxidation than does the commercial Pt–Ru/C. Methanol oxidation current density is shown to change in the order Pt–Ru–Ni/C (175 °C) > Pt–Ru–Ni/C(150 °C) ≈ Pt–Ru–Ni/C (200 °C) > Pt–Ru–Ni/C (250 °C) > Pt–Ru/C(J–M) > Pt–Ru–Ni/C (300 °C). The maximum activity for methanol oxidation was found with a heat-treatment temperature of ca. 175 °C. Indeed, other investigators have discussed the role of Ru species within the Pt–Ru systems for methanol oxidation [14,28,31]. It is broadly advanced that the presence of hydrous Ru species results in improved methanol oxidation because hydrous ruthenium oxide plays the dual role of a proton and electron conductor. As reported by Zheng et al. [38], the amount of hydrous ruthenium oxide decreases when the heat-treatment temperature exceeds 175 °C. Thus, the maximum hydrous ruthenium oxide content should be found with the heat-treatment temperatures below 175 °C. Therefore, in this paper, the activity change of methanol oxidation with the heat-treatment temperature may be attributed mainly to the change in hydrous ruthenium oxide content within the catalysts as well as (partly) to increased particle size.

To further evaluate the activity and stability of the catalysts, the catalytic electrodes were polarized at 0.35 V/SCE for a period of time. Fig. 6 shows the chronoamperomet-

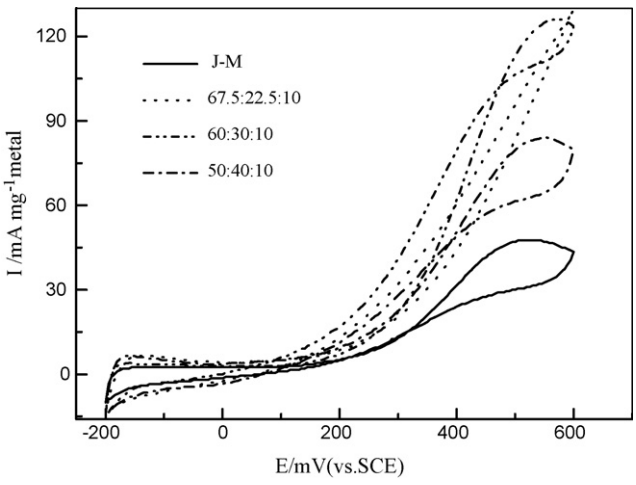

Fig. 4. CVs of as-prepared Pt–Ru–Ni catalysts with different atomic compositions, heat treated at 175 °C, and the commercial catalyst at a scan rate of 20 mV s^{-1} in 0.5 M CH_3OH + 0.5 M H_2SO_4 solution.

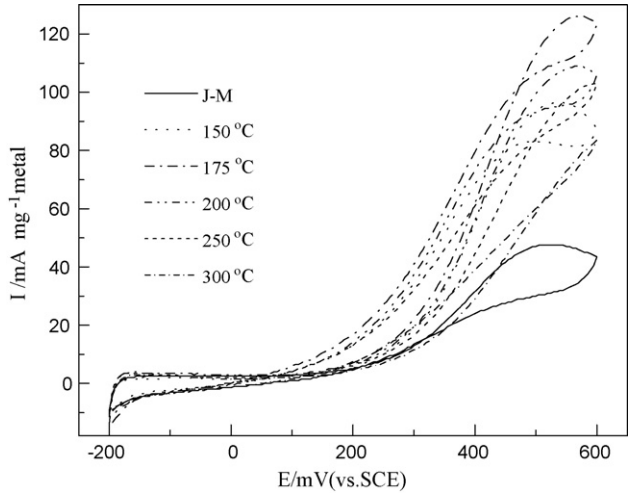

Fig. 5. CVs of methanol oxidation on the Pt–Ru–Ni(60:30:10)/C catalysts heat treated at various temperatures, and the commercial catalyst at a scan rate of 20 mV s^{-1} in 0.5 M CH_3OH + 0.5 M H_2SO_4 solution.

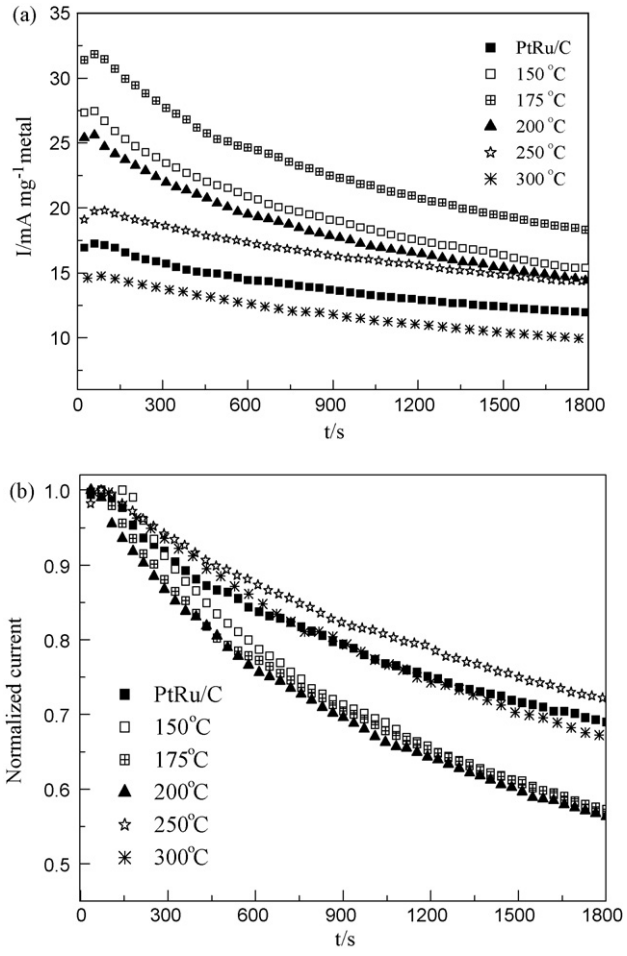

Fig. 6. (a) Chronoamperometric curves of the Pt–Ru–Ni(60:30:10)/C catalysts after heat treatment at different temperatures, and commercial catalyst in 0.5 M H_2SO_4 + 0.5 M CH_3OH at a given potential of 0.35 V and (b) their normalized current–time curves.

ric (CA) curves for methanol oxidation on homemade Pt–Ru–Ni (60:30:10)/C catalysts and the commercial PtRu/C catalyst. From Fig. 6a, it is found that the maximum oxidation current density is obtained with the Pt–Ru–Ni/C(175 °C) catalyst. The activity change for methanol oxidation decreases in the order of Pt–Ru–Ni/C (175 °C) > Pt–Ru–Ni/C(150 °C) > Pt–Ru–Ni/C(200 °C) > Pt–Ru–Ni/C(250 °C) > Pt–Ru/C(J–M) > Pt–Ru–Ni/C (300 °C), which is in fairly good agreement with our CV results. To examine the possible effect of heat-treatment temperature of the ternary catalyst on its stability for methanol oxidation, the normalized current density (i/i_{max}) versus time was plotted in Fig. 6b. For each catalytic electrode, it is found that the catalytic current density decays monotonically with time, but at different rates. For 30 min polarization, methanol oxidation currents on the Pt–Ru–Ni/C catalysts heat treated at 250 and 300 °C decrease to ca. 70% of the maximum current, which is comparable with that for the commercial Pt–Ru catalyst. In contrast, the current densities of methanol oxidation on the Pt–Ru–Ni/C catalysts heat treated at 150, 175 and 200 °C (again after 30 min polarization) decay more rapidly and attain a value for the same time period about 40% of the maximum current density. Clearly, such chronoamperometric data indicate that the stabilities of Pt–Ru–Ni/C catalysts heat treated at higher temperatures are much enhanced over catalysts heat treated at lower temperatures.

As discussed above, the maximum catalytic activity for methanol oxidation was found on a Pt–Ru–Ni(60:30:10)/C catalyst heat treated at 175 °C, whereas good stability was found for catalysis using Pt–Ru–Ni (60:30:10)/C heat treated at evaluated temperatures. It is commonly accepted that the composition, structure and particle size of Pt-based alloy electrocatalysts have a significant influence on their activity and stability of the methanol oxidation reaction. To examine any possible effects of the ternary catalyst composition on their stability, carbon-supported catalysts with different Pt–Ru–Ni atomic ratios were subject to CV measurements (15 cycles) in fresh 0.5 M H_2SO_4 and 0.5 M CH_3OH + 0.5 M H_2SO_4 solutions as shown in Figs. 3 and 4 and CA measurements in 0.5 M CH_3OH + 0.5 M H_2SO_4 solutions for 30 min as shown in Fig. 6, respectively. Both AES-ICP and additional atomic absorption spectroscopic techniques were employed to evaluate the possible dissolution of metal species. However, we could not find any dissolution of metal species (especially for Ni species) after the electrochemical measurements. As indicated by Toda et al. [39], the Pt enrichment on the surface of Pt–Ni alloy film was found at a potential of 1.1 V/RHE, due to the dissolution of Ni. Martinez-Huerta et al. [35] also reported the Ni dissolution from the Pt–Ni based alloys when cycling beyond 1 V/RHE. In the paper by Park et al. [34], the Pt–Ni alloy electrodes were first pretreated in H_2SO_4 solution over a wide potential range of 0–1.6 V/RHE, which may lead to the formation of surface redox Ni species and/or the Pt surface enrichment and thus an enhanced methanol oxidation activity. However, they did not find the dissolution of Ni species. Whereas, in this work, the potential has an upper limit of 0.6 V/SCE so that the Ni dissolution could be avoided. Thus, the rapid decline in current with time for those catalysts at heat-treatment temperatures lower than ca. 200 °C is not due to the Ni dissolution from the ternary electrocatalysts.

As referenced earlier (vide supra), Rolison et al. [14] discussed the role of hydrous ruthenium oxide in Pt–Ru catalysts for methanol oxidation. It was advanced that the hydrous ruthenium oxide, rather than Ru metal, is the most active component in Pt–Ru catalysts. Additionally, Zheng et al. [38] reported that hydrous ruthenium oxide possesses an amorphous hydrated structure below 175 °C and an anhydrous structure above 300 °C. Thus, one might infer that the maximum catalytic activity of methanol oxidation on Pt–Ru–Ni/C (175 °C) is ascribed to the formation of hydrous ruthenium oxide. On the other hand, Yu-Min Tsou et al. [32] from E-TEK asserts that hydrous ruthenium oxide plays a role in the chemical instability of the catalyst, which might explain the observed low stability of Pt–Ru–Ni/C catalysts heat treated at low temperatures; indeed, when samples were heat treated above 250 °C, one clearly observes enhanced alloying involving Pt, Ru and Ni. Consequently, the enhanced stability of the catalysts that are heat treated at evaluated temperatures may be associated with increased alloying. We conclude that the presence of alloys of Pt,

Ru and Ni provides for a rationalization of both the activity and stability of the Pt–Ru catalytic system for methanol oxidation.

4. Conclusions

In summary, study of methanol oxidation on carbon-supported Pt–Ru–Ni ternary nanoparticles has revealed details concerning the activity and stability of the catalysts. Carbon-supported Pt–Ru–Ni ternary catalysts of different atomic ratios that were heat treated at several temperatures have shown enhanced electrocatalytic activity for the oxidation of methanol, when compared to a commercial Pt–Ru alloy catalyst from Johnson–Matthey. The maximum activity of ternary catalysts for methanol oxidation was found for the Pt–Ru–Ni atomic ratio of 60:30:10 when heat treated at ca. 175 °C. However, the stability, unlike the activity, was found to be greatly improved at heat-treatment temperatures higher than ca. 250 °C, probably associated with higher alloy concentrations that occur at higher temperatures within the ternary catalysts. The significantly enhanced catalytic activity for methanol oxidation can be attributed to the high dispersion of ternary catalysts and to Ni acting as a promotion agent. We also conclude that hydrous ruthenium oxides play an important role in activity enhancement, and that the degree of alloying within the catalyst is a crucial factor in determining good stability of the Pt–Ru based catalysts; this latter conclusion helps in answering the apparent conflicting dependency of the activity and stability on the temperature for methanol oxidation using Pt–Ru electrocatalysts.

Acknowledgments

The authors would like to thank the GF Fundamental Foundation of China (A1320070025), the National "863" High-Technology Research Program of China (2006AA05Z136 and 2006AA04Z342), the National Natural Science Foundation of China (20673136), the 100 People Plan Program of the Chinese Academy of Sciences and the Pujiang Program of Shanghai City (No. 06PJ14110) for support of this work.

References

[1] A.S. Arico, S. Srinivasan, V. Antonucci, Fuel Cells 2 (2001) 133.
[2] S. Wasmus, A. Kuver, J. Electroanal. Chem. 461 (1999) 14.
[3] B.D. McNicol, D.A.J. Rand, K.R. Williams, J. Power Sources 83 (1999) 15.
[4] S.C. Kelley, G.A. Deluga, W.H. Smyrl, Electrochem. Solid-State Lett. 3 (1999) 407.
[5] X.M. Ren, S. Zelenay, S. Thomas, J. Davey, S. Gottesfeld, J. Power Sources 86 (2000) 111.
[6] P.S. Kauranen, E. Skou, J. Electroanal. Chem. 408 (1996) 189.
[7] B. Gurau, E.S. Smotkin, J. Power Sources 112 (2002) 339.
[8] J.J. Huang, H. Yang, Q.H. Huang, Y.W. Tang, T.H. Lu, D.L. Akins, J. Electrochem. Soc. 151 (2004) 1810.
[9] Z.B. Wang, G.P. Yin, P.F. Shi, Y.C. Sun, Electrochem. Solid-State Lett. 9 (2006) 13.
[10] J. McBreen, S. Mukerjee, J. Electrochem. Soc. 142 (1995) 3399.
[11] M. Watanabe, S. Motoo, J. Electroanal. Chem. Interfacial Electrochem. 60 (1975) 267.
[12] M. Neergat, D. Leveratto, U. Stimming, Fuel Cells 2 (2002) 25.
[13] T.J. Schmidt, M. Noeske, H.A. Gasteiger, B.J. Behm, Langmuir 13 (1997) 2591.
[14] D.R. Rolison, P.L. Hagans, K.E. Swider, J.W. Long, Langmuir 15 (1999) 774.
[15] H.A. Gasterger, N. Markovic, P.N. Ross, E.J. Cairns, J. Phys. Chem. 97 (1993) 12020.
[16] W. Chrzanowski, A. Wieckowski, Langmuir 14 (1998) 1967.
[17] P.K. Shen, A.C.C. Tseung, J. Electrochem. Soc. 141 (1994) 3082.
[18] A.S. Arico, Z. Poltarzewski, H. Kim, V. Antonucci, J. Power Sources 55 (1995) 159.
[19] M. Gotz, H. Wendt, Electrochim. Acta 43 (1998) 3637.
[20] F. Colmati, E. Antolini, E.R. Gonzalez, Electrochim. Acta 50 (2005) 5496.
[21] W. Napporn, H. Laborde, J.M. Leger, C. Lamy, J. Electroanal. Chem. 404 (1996) 153.
[22] K.L. Ley, R. Liu, C. Pu, Q. Fan, N. Leyarovska, C. Segre, E.S. Smotkin, J. Electrochem. Soc. 144 (1997) 1543.
[23] A.S. Aricò, S. Srinivasan, V. Antonucci, Fuel Cells 2 (2001) 133.
[24] H.A. Gasteiger, N. Markovic, P.N. Ross, E.J. Cairns, J. Electrochem. Soc. 141 (1994) 1795.
[25] C. Lamy, A. Lima, V. LeRhun, F. Delime, C. Coutanceau, J.M. Léger, J. Power Sources 105 (2002) 283.
[26] J.C. Huang, Z.L. Liu, C.B. He, L.M. Gan, J. Phys. Chem. B 109 (2005) 16644.
[27] H.N. Dinh, X.M. Ren, F.H. Garzon, P. Zelenay, S. Gottesfeld, J. Electroanal. Chem. 491 (2000) 222.
[28] J.W. Long, R.M. Stroud, K.E. Swider-Lyons, D.R. Rolison, J. Phys. Chem. B 104 (2000) 9772.
[29] (a) R.K. Raman, A.K. Shukla, A. Gayen, M.S. Hegde, K.R. Priolkar, P.R. Sarode, S. Emura, J. Power Sources 157 (2006) 45;
(b) C. Bock, A. Collier, B. MacDougall, J. Electrochem. Soc. 152 (2005) 2291.
[30] Y.Q. Xu, X.F. Xie, J.W. Guo, S.B. Wang, Y.W. Wang, V.K. Mathur, J. Power Sources 162 (2006) 132.
[31] Q.Y. Lu, B. Yang, L. Zhuang, J.T. Lu, J. Phys. Chem. B 109 (2005) 1715.
[32] Y.M. Tsou, Z.Y. Zhu, L.X. Cao, E.D. Castro, 187th ECS Meeting, 2004-ecsmeet1.peerx-press. Org.
[33] J.H. Choi, K.W. Park, B.K. Kwon, Y.E. Sung, J. Electrochem. Soc. 150 (2003) 973.
[34] (a) K.W. Park, J.H. Choi, B.K. Kwon, S.-A. Lee, Y.E. Sung, H.Y. Ha, S.A. Hong, H. Kim, A. Wieckowski, J. Phys. Chem. B 106 (2002) 1869;
(b) K.W. Park, J.H. Choi, Y.E. Sung, J. Phys. Chem. B 107 (2003) 5851.
[35] M.V. Martinez-Huerta, S. Rojas, J.L. Gomez de la Fuente, P. Terreros, M.A. Pena, J.L.G. Fierro, Appl. Catal. B: Environ. 69 (2006) 75.
[36] Y.M. Liang, H.M. Zhang, Z.Q. Tian, X.B. Zhu, X.L. Wang, B.L. Yi, J. Phys. Chem. B 110 (2006) 7828.
[37] (a) A.J. Dickinson, L.P.L. Carrette, J.A. Collins, K.A. Friedrich, U. Stimming, Electrochim. Acta 47 (2002) 3733;
(b) N. Alonso-Vante, Fuel Cells 6 (2006) 182;
(c) J.Y. Cao, C. Du, S.C. Wang, P. Mercier, X.G. Zhang, H. Yang, D.L. Akins, Electrochem. Commun. 9 (2007) 735.
[38] J.P. Zheng, P.J. Cygan, T.R. Jow, J. Electrochem. Soc. 142 (1995) 2699.
[39] T. Toda, H. Igarashi, M. Watanabe, J. Electrochem. Soc. 145 (1998) 4185.